X-ray Microbeam Investigation of Deformation Microstructure in Microindented Cu

Wenge Yang[1], B. C. Larson[1], G. M. Pharr[1,2], G. E. Ice[1], J. Z. Tischler[1], J. D. Budai[1], and Wenjun Liu[1]
[1]Oak Ridge National Laboratory, Oak Ridge, Tennessee 37831
[2]University of Tennessee, Knoxville, Tennessee 37996

ABSTRACT

The deformation microstructure under spherical microindents in single crystal Cu has been investigated with submicron spatial resolution using x-ray structural microscopy. A polychromatic, submicron diameter (~0.5 μm) microbeam was used in combination with micron-resolution depth profiling to make direct, nondestructive measurements of plastic deformation induced lattice rotations under an indent made with a 69 μm radius spherical indenter and 200 mN maximum load. Lattice orientations relative to the undeformed crystal were determined as a function of position under the indent using differential-aperture x-ray structural microscopy (DAXM). Rotation-axes and misorientation-angles were determined for micron steps along selected microbeam penetration directions.

INTRODUCTION

Indentation experiments have long been used as a characterization tool for evaluating mechanical properties from small volumes of material [1,2]. In the last few years, strain-gradient concepts have been inserted into continuum plasticity theory to explain the observation of a significant impact of indenter shape and penetration depth on microhardness measurements. These effects have presented a challenge to computer simulation and modeling as well as continuum theory as indenters with different shapes (i.e. Berkovich, spherical, conical) yield depth and shape dependent hardness results. Conical and Berkovich indentation measurements display depth dependent hardness, while spherical indentations show indenter radius dependent hardness [3,4]. Dislocations associated with plastic deformation are known to self-assemble into well-developed patterns of geometrically necessary dislocation (GND) and statistically stored dislocation distributions [5,6]. A detailed knowledge of the dislocation microstructure and an understanding of the fundamental processes and microscopic mechanisms associated with plastic deformation are keys to understanding the underlying source of indent geometry specific hardness results. Transmission electron microscopy (TEM) [7-9], electron backscattering diffraction microscopy [10], and atomic force microscopy [11] have been used to investigate the induced dislocation microstructure, the generation of surface steps, and pile-up around indent tips. These techniques provide important information regarding the microstructure under nanoindents; however, a comprehensive understanding of indent hardness measurements and the underlying crystal lattice deformation process in bulk materials is not yet available. Additional three-dimensional measurements of the local microstructure in bulk materials are needed to provide a detailed quantitative description of deformation for critical comparison with computer simulations and modeling.

The capability to make grain average deformation measurements with ~5-10 μm spatial resolution has been developed [12,13] using high-energy x-ray microbeams. This technique has provided insight into polycrystalline deformation modes [13] and increasingly powerful

techniques are being developed. However, nondestructive 3D microstructural measurements with the submicron, point-to-point spatial resolution required for investigation of the heterogeneous intra-granular deformation below nanoindents have only recently become available [14].

In the work presented here, we have used Kirkpatrick-Baez x-ray focusing mirrors and differential-aperture diffracted beam profiling to determine local misorientations and rotation axes from submicron volume elements below a 200 mN spherical indent in single crystal copper. This provides a powerful tool for nondestructive study of the local microstructure and plastic deformation that is complementary to TEM.

EXPERIMENT

The microbeam diffraction geometry used for these measurements is shown schematically in Fig. 1. A white x-ray microbeam enters the indented surface with an angle of 45 degrees to the surface normal and penetrates to depths as large as ~ 50 µm before being absorbed photo-electrically or diffracted by the crystal lattice into the CCD area detector. As discussed elsewhere [14], by collecting CCD images before and after submicron steps of a 50 µm Pt profiling wire along the sample surface, differential intensity distributions can be used to triangulate from the pixel position of the intensity to the wire position and then extrapolate to determine the source of intensity along the microbeam. Computer collation of this differential intensity distribution for each wire step along the sample surface makes it possible to reconstruct full Laue diffraction images from submicron voxels along the penetration direction. As a result, complete white-beam diffraction patterns are obtained for each segment of material along the penetration direction of the x-ray microbeam. The resulting depth resolved Laue diffraction patterns provide spatially resolved measurements of the plastic deformation microstructure along the microbeam. Three dimensional arrays of these point-to-point intra-granular measurements provide the information necessary to determine GND distributions.

A 69 µm radius spherical indenter was used to make 200 mN maximum load indents into a dislocation free Cu single crystal with a <111> surface normal. The Cu crystal was oriented such that a <110> type axis is normal to the plane of Fig. 1 and a <112> type axis is along the trace of the surface in the figure.

Contrary to Berkovich, conical or Vickers indenters, spherical indenters have constant curvature at all contact points, so only the anisotropic elastic properties and the crystal lattice geometry impact the symmetry of the deformation. In this short paper we report measurements

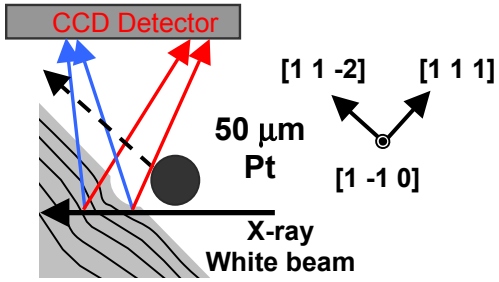

Figure 1. Schematic of the 3D x-ray microscope, sample, beam, and profiler.

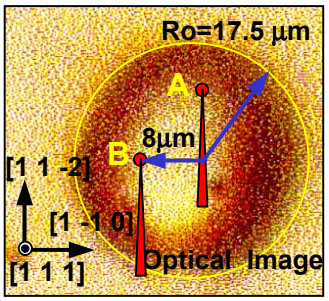

Figure 2. Optical micrograph of 200 mN Spherical indent in Cu. The A and B positions, the microbeam direction, and microbeam entry points are shown.

at two locations; one measurement within the center plane of the indent and another at a point displaced laterally from the center point, as indicated by positions A and B in Fig. 2, respectively. At position A (within the central symmetry plane), the x-ray microbeam enters the sample inside the contact radius and penetrates the sample for ~50 µm. This takes the beam significantly outside and below the contact area. At position B, the beam again enters the sample within the contact radius, but from this position it cuts through radial planes with continuously varying angles as the microbeam penetrates ~ 50 µm along the 45 degree direction into the sample. To the extent that the external force is along the radial direction at the contact surface, all the points measured at the A position are on the same radial plane. For position B, each point is on a different radial plane so volume elements along this line experience continually varying external force directions.

RESULTS

Figure 3 is a composite showing the full Laue diffraction pattern at position A for the <111> oriented Cu crystal in panel (b) and an expanded view of the elongated (hhh) reflection in panel (a). Overall the nearly vertical direction of the (hhh) reflection streak shows that the lattice is rotated around an axis parallel to the [1-10] direction (i.e., horizontal direction). Since white

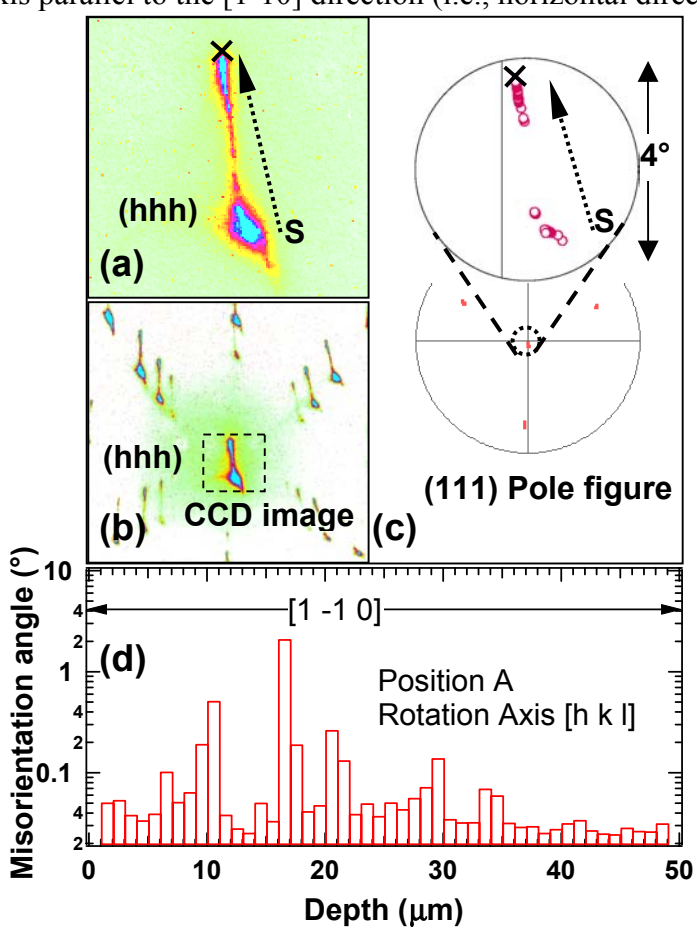

Figure 3. Enlarged (hhh) Laue pattern (a) and full Laue pattern (b) at sample position A. (c) depth resolved (111) pole figure; (d) log plot of local misorientation angles at position A as a function of penetration depth with nominal rotation axis [1 -1 0] indicated.

beam Laue patterns represent a one-to-one mapping of local plane orientations onto the CCD area detector [17], this shows that the deformation along the beam in this plane corresponds to the lattice plane rotating around a [1 -1 0] lattice direction. The distribution of lattice rotations as a function of depth along the microbeam is clearly heterogeneous, as the intensity distribution of the streak shows a qualitatively uneven distribution. Figure 3c represents a (111) depth dependent pole figure, where the inset provides an enlarged view of the central (111) pole as a function of depth. The open circles represent micron resolution measurements of the lattice rotation as a function of depth along the beam. The arrows in Fig. 3a and 3c show the direction of progression with depth and the correspondence between the Laue pattern and the lattice orientation. The peak in intensity toward the bottom of the image corresponds to ~15 microns of depth near the crystal surface that have small relative rotations; there is then a rapid orientation change before returning slowly to the undistorted crystal position denoted by the "X". The local misorientation angles (i.e. local orientation compared to the orientation of the following μm) are plotted as a function of depth in Figure 3(d). As implied above, the rotation axis lies close to the [1 -1 0] direction for all positions along the microbeam. Noting the log scale for the rotations in Fig. 3d, there are 15 microns over which the total rotation is ~1.5 degrees; there is then a rather large ~2 degree rotation followed by rotations that are a few tenths of degrees or smaller per micron.

Measurements and analyses analogous to those for position A are shown for position B in Fig. 4. As was the case for position A, the intensity distribution is inhomogeneous for position B; however, the angular distribution of the intensity at position B is quite different. It contains rotations around several axes, as might be expected as the beam encounters regions on different radial deformation planes. The distribution of intensity in Fig. 4a appears to be somewhat more homogeneous than that in Fig. 3a; this is reflected in the distribution of angular steps in Figs. 4c and 4d. The arc shaped form of the intensity and the (111) pole figure indicates immediately that, unlike the case for position A, the axes of rotation change significantly with depth along the beam penetration direction. The rotation axes are shown quantitatively in Fig. 4d, where not only the magnitude of the (micron-by-micron) misorientations, but also the directions of the rotation axes are shown to change markedly. Initially (i.e. near the sample surface at position B), the rotation axis is along the [-4 3 2] direction; the rotation axis then changes to the [-2 -3 4] direction and subsequently to the [-2 -3 0] direction before settling into the [1 -1 1] direction for the last ~25 μm.

DISCUSSION

These measurements emphasize that it is possible to make submicron point-to-point microstructural orientation measurements at arbitrary positions below nanoindents. The depth dependence of the rotations shows that the spatial extent of the deformation field continues much further than the contact hemisphere, which extends only ~15 μm along beam at positions A and B. As was the case with previously reported measurements under a Berkovich indent in this same copper sample [16], the total rotation immediately under the indenter faces are around an axis corresponding to the indented surface tangent in the plane of the crystal surface, as expected. As determined by the position of the first point in Figs. 3d and 4d relative to the (hhh) point, the axes correspond to the [1-1 0] direction at point A and the [-1-1 2] direction at point B for the spherical indent. Measurements have been made at similar locations in 100 mN

maximum load Berkovich indents [16]; the rotation axes for Berkovich indents correspond (approximately) to the [1-1 0] direction at point A and the [1 0-1] direction at point B.

For the case of the micron-by-micron local misorientation axes (Fig. 3d), both the spherical and Berkovich indents retain the [1-1 0] axes for all depths at position A. On the other hand, the Berkovich and spherical indent results for position B (Fig. 4d) differ significantly regarding the crystallographic axes of the local rotations along the microbeam. While the rotation axes for the first ~10 µm at position B in the spherical indent case shown in Fig. 4d are [-4 3 2], the rotation axis for the first four microns at this position for the Berkovich indent was along the [1 0 -1] direction [16], apparently driven by the rotation angle of the flat face. The directions of misorientation axes become rather complicated for depths below 10 µm for spherical indents at position B; however, the rotations tend to fall around three axes, the [-2-3 4], [-2 -3 0], and [1-1 1] directions. For the Berkovich case at position B, a single step rotation of ~6 degrees around the [3 2-3] axis was followed by rotations around the [1-2 0] and the [1-1 0] axes. In general, the differences in the local rotation axes for the two types of indenters indicate differences in the spatial distribution of active slip systems for the spherical and Berkovich indenters that will be important in connection with computer simulations and modeling.

Although one dimensional estimate of the density of geometrically necessary dislocations can be obtained from the lattice rotations measured along the microbeam at these two positions,

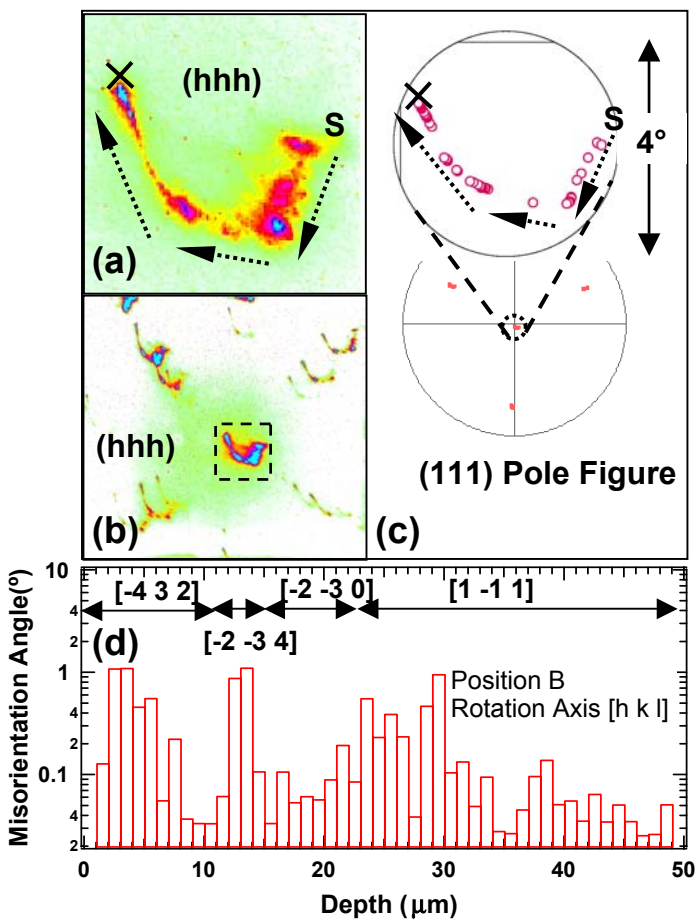

Figure 4. Enlarged (hhh) Laue pattern (a) and full Laue pattern (b) at sample position B. (c) depth resolved (111) pole figure; (d) log plot of local misorientation angles at position B as a function of penetration depth.

such analyses will be discussed in subsequent publications. We comment in closing that detailed measurements of the local lattice rotation magnitudes and rotation axes over the entire 3D volumes deformed by the indenters are needed to fully specify deformation distributions for detailed comparisons with computer simulations and multi-scale modeling.

CONCLUSIONS

Nondestructive, 3D measurements of the deformation microstructure under a spherical indent in Cu have been made with submicron-resolution using x-ray structural microscopy. Spatially resolved measurements of local orientations performed along a plane of symmetry and along an off-symmetry direction show dramatically different lattice rotations in accordance with qualitative expectations. Comparison of the axes of lattice rotations with similar measurements for Berkovich indents indicates the near surface (~5-10 μm) deformation induced rotations to be dominated by the indenter shape.

ACKNOWLEDGMENTS

Research sponsored by the Department of Energy, Office of Science, Division of Materials Sciences at ORNL managed by UT-Battelle, LLC, under contract DE-AC05-00OR22725. Work was performed on the UNI-CAT beamline at the APS; the operation of the APS is sponsored by the DOE; operation of UNI-CAT is supported UIUC-MRL, ORNL, NIST, and UOP Res., Inc.

REFERENCES

[1] J.B. Thompson, J. H Kindt, B. Drake, H.G. Hansma, D.E. Morse and P.K. Hansma, *Nature*, **414**, 773 (2001).
[2] B.R. Lawn, N.P. Padture, H.D. Cai and F. Guiberteau, *Science*, **263**, 1114 (1994).
[3] J.G. Swadener, E.P. George, G.M. Pharr, *J. Mech Phys. Solids*, **50**, 681 (2002).
[4] Z. Xue, Y. Huang, K.C. Hwang and M. Li, *J. Eng. Mater–T ASME*, **124**, 371 (2002).
[5] D.A. Hughes and N. Hansen, *Acta Mater.*, **45**, 3871 (1997).
[6] E. Van der Giessen and A. Needleman, *Script Mater.*, **48**, 127 (2003).
[7] Q. Ma and D.R. Clarke, *J. Mater. Res.*, **10**, 853 (1995).
[8] J.E. Bradby, J.S. Williams, J. Wong-Leung, M.V. Swain and P. Munroe, *Appl. Phys. Lett.*, **77**, 3749 (2000).
[9] I. Zarudi, J.Zou and L.C. Zhang, *Appl. Phys. Lett.*, **82**, 874(2003).
[10] D.F. Bahr, K.A. Nibur, K.R. Morasch and D.P. Field, *JOM*, **55**(2), 47 (Feb. 2003).
[11] S. Harvey, H. Huang, S. Venkataraman and W.W. Gerberich, *J. Mater. Res*. **8**, 1291 (1993).
[12] H.F. Poulsen, S.F. Nielsen, E.M. Lauridsen, S. Schmidt, R.M. Suter, U, Lienert, U. L. Margulies, T. Lorentzen, and D.Juul Jensen, *J. Appl. Cryst*. **34**, 751 (2001).
[13] L. Margulies, G. Winther, and H.F. Poulsen, *Science* **292**, 2392 (2001).
[14] B.C. Larson, W. Yang, G.E. Ice, J.D. Budai and J.Z. Tischler, *Nature*, **415**, 887 (2002).
[15] G.E. Ice and B.C. Larson, *Adv. Eng. Mat.*, **2**, 643 (2000).
[16] W. Yang, B.C. Larson, G.M. Pharr, G.E. Ice, J.G. Swadener, J.D. Budai, J.Z. Tischler and W. Liu, *Mat. Res. Soc. Symp. Proc*. **750**, Y8.26 (2003).
[17] R. Barabash, G.E. Ice, B.C. Larson, G.M. Pharr, K.-S. Chung, and W. Yang, *Appl. Phys. Lett.***79**, 4 (2001).